Core-Shell Construction of Metal@Carbon by Mechanochemically Recycling Plastic Wastes: Towards Efficient Oxygen Evolution Reaction

Jiahua Zhao[a], Qiang Niu[b], Junjun Zhang[c] and Pengfei Zhang[a, c*]*

[a.] School of Chemistry and Chemical Engineering, Shanghai Jiao Tong University, Shanghai 200240, P. R. China.

[b.] National enterprise technology center, Inner Mongolia Erdos Electric Power and Metallurgy Group Co., Ltd., Inner Mongolia 016064, P. R. China

[c.] State Key Laboratory of High-efficiency Utilization of Coal and Green Chemical Engineering, College of Chemistry and Chemical Engineering, Ningxia University, Yinchuan 750021, P. R. China.

Correspondence: chemistryzpf@sjtu.edu.cn, zhangjj089@nxu.edu.cn

1. Materials and Experimental

1.1. Materials

Nickel nitrate hexahydrate ($Ni(NO_3)_2 \cdot 6H_2O$), iridium dioxide (IrO_2), ethanol (C_2H_5OH), and Nafion (5 wt %) were purchased from Sinopharm Chemical Reagent Co., Ltd. Milli-Q ultrapure water was used for all experiments. All chemicals were analytical grade and were used as received without further purification.

Ni@Plastics-BM: 1 g of plastics powder and 1mmol ($Ni(NO_3)_2 \cdot 6H_2O$) were thoroughly mixed by ball milling for 1h. The mixture was then transferred into a cube and placed in a muffle furnace, then heated up to the 850 ℃ at the rate of 2 °C /min under N_2 for 2 h. Samples prepared from this procedure were denoted as Ni@PMMA/PBT-BM, where PMMA/PBT represents the plastic types.

Ni@Plastics-PM: 1 g of plastic powder and 1mmol ($Ni(NO_3)_2 \cdot 6H_2O$) were simply physically mixed with no ball milling. The mixture was then transferred into a cubical and placed in a muffle furnace, then heated up to the 850 ℃ at a rate of 2 °C/min under N_2 for 2 h. Samples prepared from this procedure were denoted as Ni@PMMA/PBT-PM, where PMMA/PBT represents the plastic types.

Ni@C: Carbon black powder was added to the solution with $Ni(NO_3)_2 \cdot 6H_2O$ dissolved. After stirring for 2h, the mixture was dried overnight and transferred to a cube and placed in a muffle furnace, then heated up to the 850 ℃ at a rate of 2 °C/ min under N_2 for 2 h. The loading amount of Ni was 25%.

Ni_xO_y: The precursor ($Ni(NO_3)_2 \cdot 6H_2O$) powders are also calcined at 850 °C in N_2 to prepare Ni_xO_y catalysts without C.

Ni@ Plastics-wet impregnation*:* The precursor ($Ni(NO_3)_2 \cdot 6H_2O$) powders were dissolved in water, and then plastic powder was added. The solution stirred for 1 hour and then H_2O evaporated using a rotary evaporator, and finally heated up to the 850 ℃ at the rate of 2 °C/min under N_2 for 2 h. The loading amount of Ni was 25%.

C@PBT: The precursor PBT powders are also calcined at 850 °C in N_2 to prepare carbon catalysts without $Ni(NO_3)_2 \cdot 6H_2O$.

1.2 Characterization

Nitrogen adsorption isotherms were measured usding an ASAP 2460 sorption analyzer (Micromeritics). The Brunauer–Emmett–Teller (BET) method was utilized to calculate the specific surface areas (SBET). Pore size distributions (PSDs) were determined from the adsorption branches of the isotherms using Density Functional Theory (DFT) and the Barrett–Joyner–Halenda (BJH) model for micropores and mesopores, respectively. Total pore volumes (Vtotal) were calculated from the amount adsorbed at a relative pressure, P/P_0 of 0.99. Micropore volumes (Vmicro) were calculated using the t-plot method.

X-ray diffraction (XRD) patterns of the samples were recorded with a Mini Flex 600 using Cu Kα radiation. Transmission electron microscope (TEM) images of the samples were obtained with an FEI Talos F200x electron microscope. Samples were dispersed on the copper mesh with ethanol. Scanning electron microscope (SEM) investigations were carried out with the JSM-7500 instrument. Raman spectra were obtained by Horiba Lab RAM HR Evolution. Fourier transform infrared reflectance (FTIR) spectra and Raman spectra were recorded on a Spectrum 100 FTIR spectrometer (PerkinElmer Inc) and DXR (Thermo Fisher) with a 532 nm laser, respectively. X-ray photoelectron spectra (XPS, Kratos Axis Ultra DLD) were conducted where XPS were recorded

with a pass energy of 160 eV and high-resolution spectra were recorded with a pass energy of 40 eV. The Ni weight loading of samples were measured by the iCAP7600 Inductively Coupled Plasma-Optical Emission Spectroscopy (ICP-OES).

The TGA experiments of the $Ni(NO_3)_2 \cdot 6H_2O$-Plastics mixture were carried out by using a Netzsch STA-449F3 TGA analyzer. In each trial, a sample of approximately 8 mg was placed into an alumina crucible and heated up to the target temperatures (1000 °C) at a stable heating rate (10 K/min) with N_2 flow of 120 mL/min. TGA analyses were used to quantitatively determine the weight changes of the PMMA/ $Ni(NO_3)_2 \cdot 6H_2O$ composites as well as their thermal stability.

O_2 temperature-programmed desorption (O_2-TPD) experiments were performed using a Beijing Builder PCA^{-1}200 analyzer with a thermal conductivity detector (TCD). About 0.2 g of each sample was heated to 300 °C with a heating rate of 10 °C/ min under flowing pure He, and held at this temperature for 3 h. After cooling the sample to 50 °C for O_2 adsorption, the gas was switched to pure He gas until the baseline was stable. The O_2-TPD measurement was then performed up to 600 °C with a ramp of 10 °C /min in flowing He (30 mL/min). Before the TCD detector, the outlet gas was passed through a pipe containing NaOH powder and cooled by an ice-salt bath to remove possible water vapor and carbon dioxide.

2. Electrochemical measurements

All the electrochemical measurements were performed in a standard three-electrode cell at room temperature using an electrochemical workstation (CHI660E), in which the sample to be tested was used as the working electrode (geometric area: 1 cm^2), a carbon rod as the counter electrode, and a Hg/HgO electrode (MOE, filled with 1 mol/L KOH solution) as the reference electrode. Electrodes for OER were prepared by uniformly casting 100 μL of catalysts-H_2O/ethanol-Nafion suspension (5 mg catalyst, 350 μL of deionized water, 700 μL of ethanol, 80 μL of 5% Nafion,) on carbon cloth (1 cm^{-2}) after ultrasound for 30 min. All linear sweep voltammetry (LSV) curves for the OER were obtained at a scan rate of 5 mV/s. The potentials were converted to the potentials referring to the RHE, according to E(*RHE*) = E(*MOE*) + 0.059 pH + 0.098 V. Tafel plots were recorded with the linear portions at low overpotential fitted to the Tafel equation.

Tafel slopes are calculated based on the equation:

$\eta = b\log j$

Where η is the overpotential, b is the Tafel slope and j is the current density.

The intercept on the real axis and the semicircle in the Nyquist plot are considered as the resistance of electrolyte (R_s) and the charge transfer resistance (R_{ct}), respectively. The equivalent circuit consists of a capacitor and a resistor in parallel. Electrochemical impedance spectroscopy (EIS) measurements were conducted at an overpotential of 500 mV with a potential perturbation amplitude of 5 mV in the range of 10 kHz to 0.1 Hz. The electrolyte resistance was measured using EIS and used for iR compensation using the equation, $E_{iR\text{-}corrected} = E_{original} - (I \times R_s)$. The ECSAs were estimated by cyclic voltammetry (CV) in the potential range of 0.989–1.139 V versus RHE without faradaic current at scan rates of 10, 20, 30, 40, 50, 60, 70, 80, 90, 100 mV s^{-1}, respectively. The current density differences [Δj = (ja − jc)] were plotted against scan rates, a linear trend was constructed.

Figures:

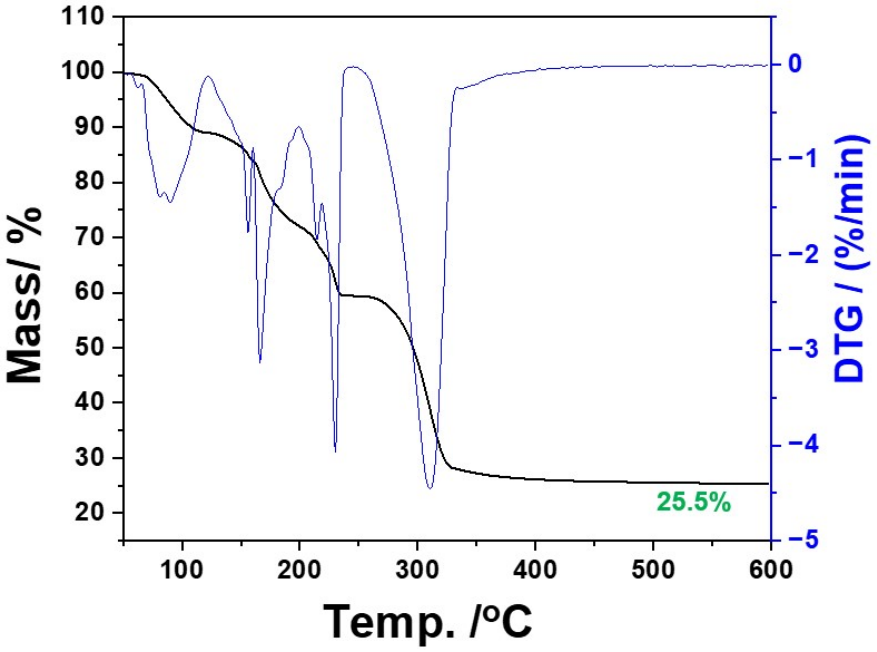

Figure S1. Thermogravimetric analysis (TGA) curve and (DSC) curve of $Ni(NO_3)_2 \cdot 6H_2O$. (under nitrogen atmosphere, 150 mL/min, from 30 to 600 °C with an increasing temperature rate of 5 °C/min).

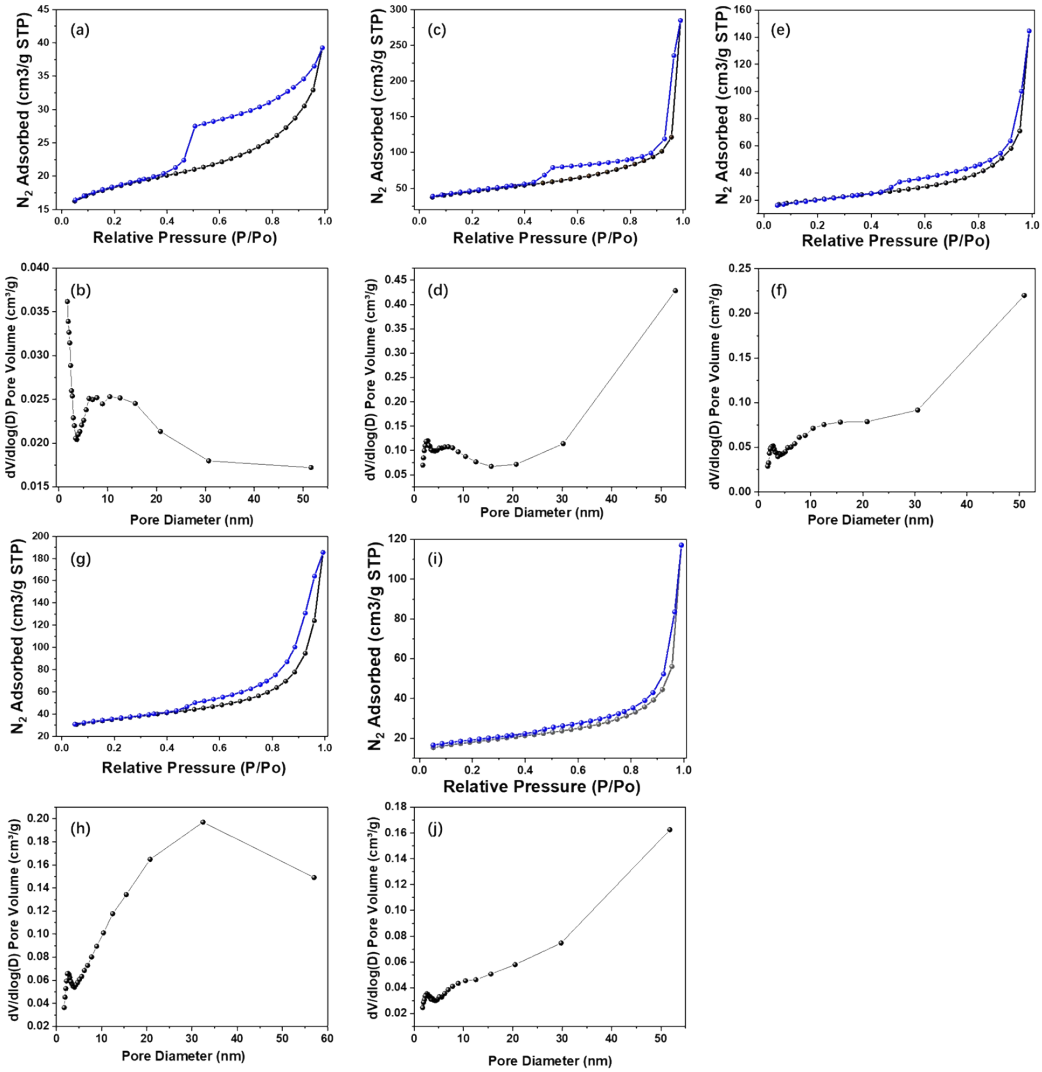

Figure S2. N_2 adsorption–desorption isotherms and pore size distribution curves of (a, b) Ni@PMMA-BM, (c, d) Ni@PBT-BM, (e, f) Fe@PBT-BM, (g, h) Co@PMMA-BM, (i, j) Mn@PBT-BM.

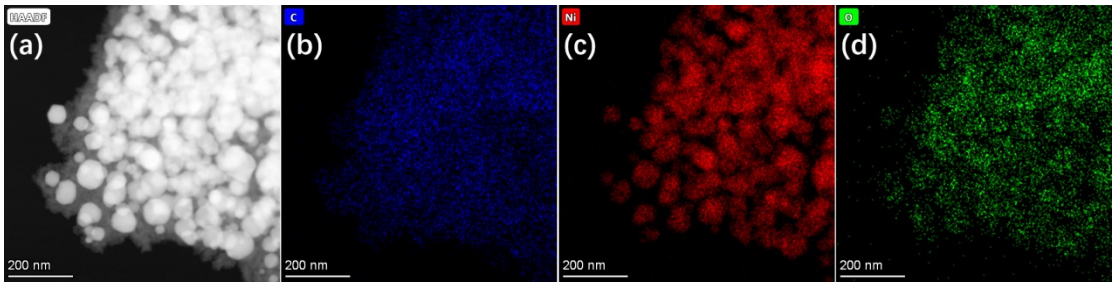

Figure S3. HAADF and EDS elemental mapping Ni@PMMA-PM (a-d). b: C, c: Ni and d: O.

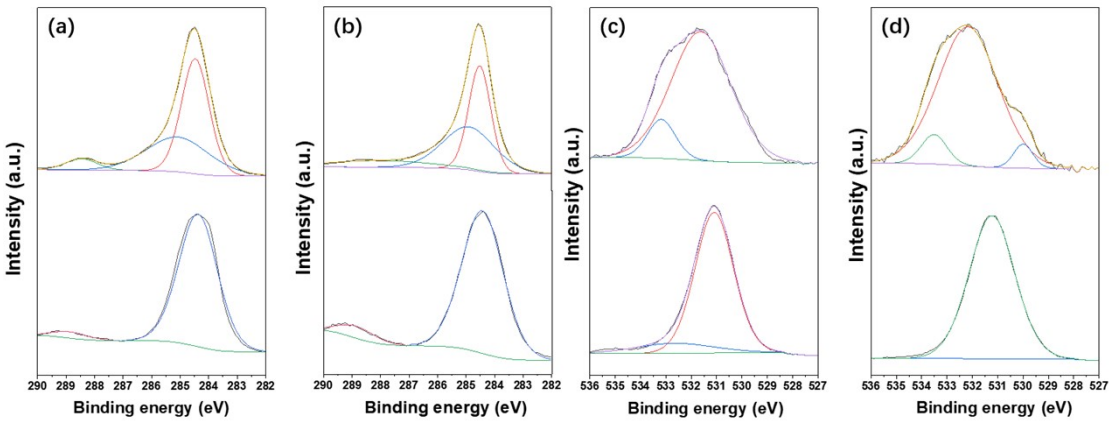

Figure S4. The high-resolution XPS spectra C 1s and O 1s of (a) Ni@PMMA-BM, (b) Ni@PMMA-CV-BM, (c) Ni@PBT-BM and (d) Ni@PBT-BM -CV. The'–CV' represents the treatment after 1000 CV cycles.

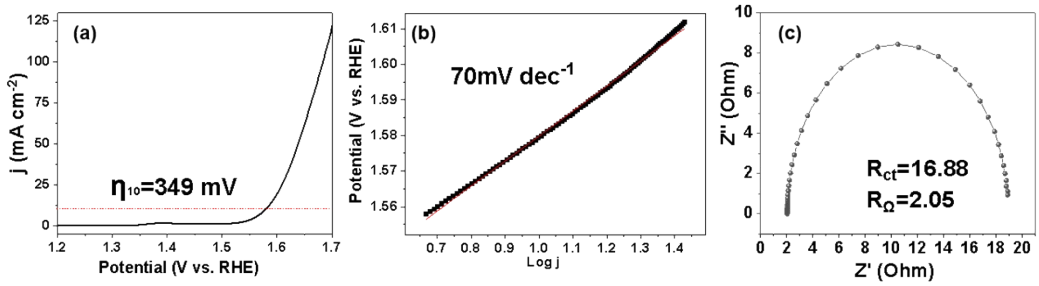

Figure S5. Ni@PMMA-wet impregnation:(a) OER LSV curves of as-prepared samples in 1M KOH with a scanning rate of 5 mV s^{-1} and corresponding OER potentials to the current density of 10 mA cm^{-2}; (b) Tafel slopes; (c) Electrochemical impedance spectrum (EIS) and the electrolyte resistance (R_Ω) and charge transfer resistance (R_{ct}).

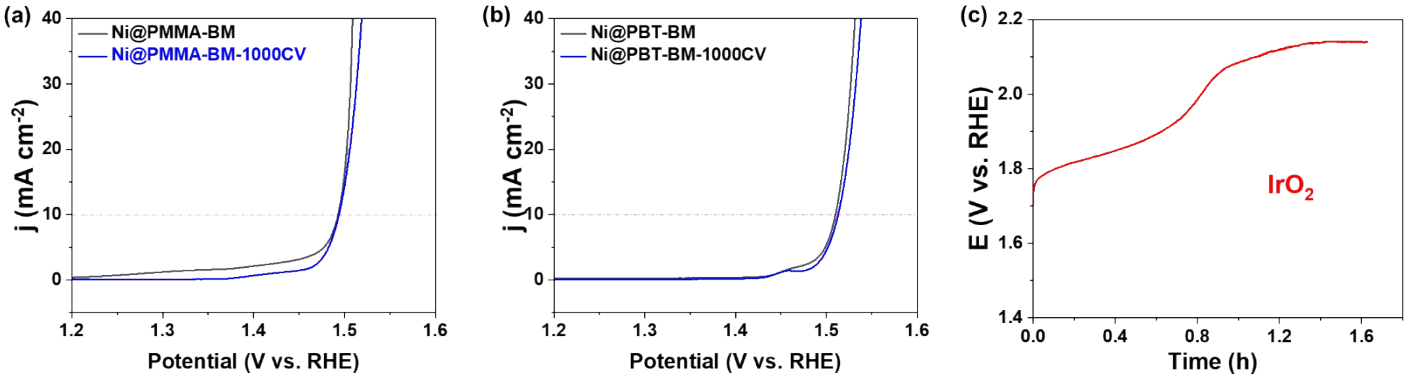

Figure S6. (a-b) OER LSV curves of as-prepared samples before and after 1000 CV cycles, (c) chronopotentiometry curve (V–t) of IrO_2 at 10 mA cm^{-2} current density.

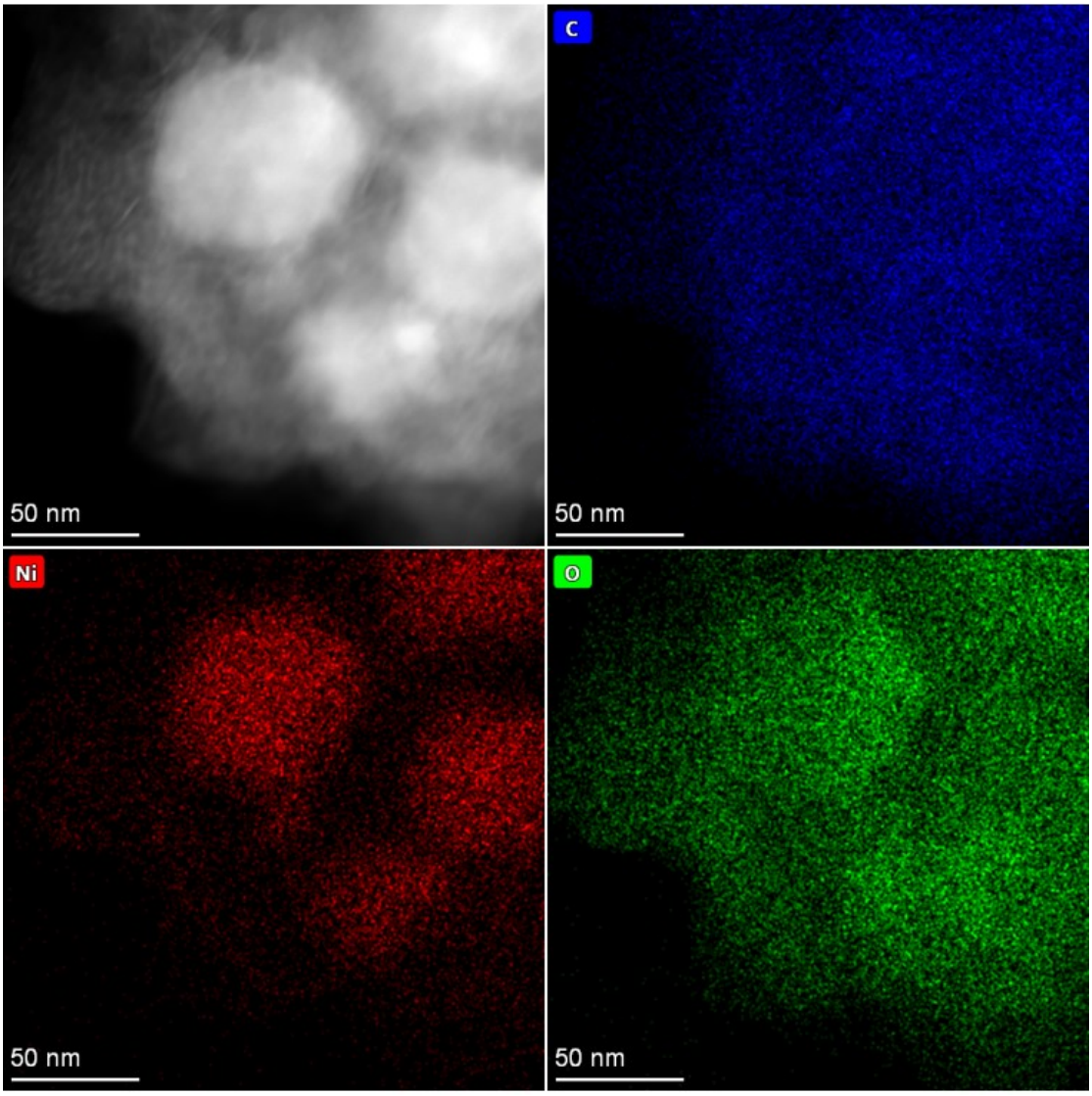

Figure S7. TEM imagesandEDS Mapping of Ni@PMMA-BM after the electrochemical stability measurement.

Note: After the electrochemical stability measurement, no metal agglomeration appears in Ni@PMMA-BM.

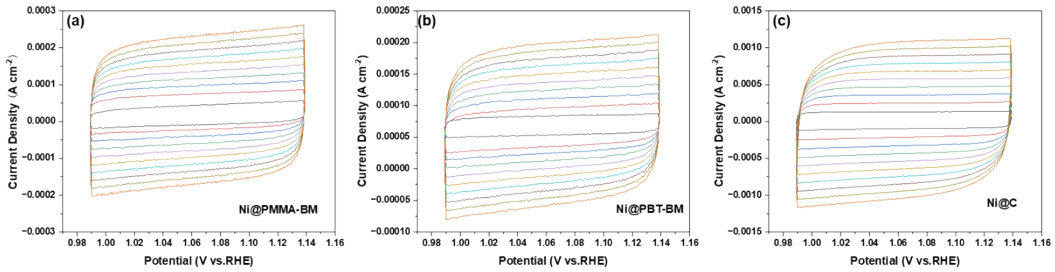

Figure S8. CV curves of different samples at scan rates of 10, 20, 30, 40, 50, 60, 70, 80, 90, and 100 mV s^{-1}.

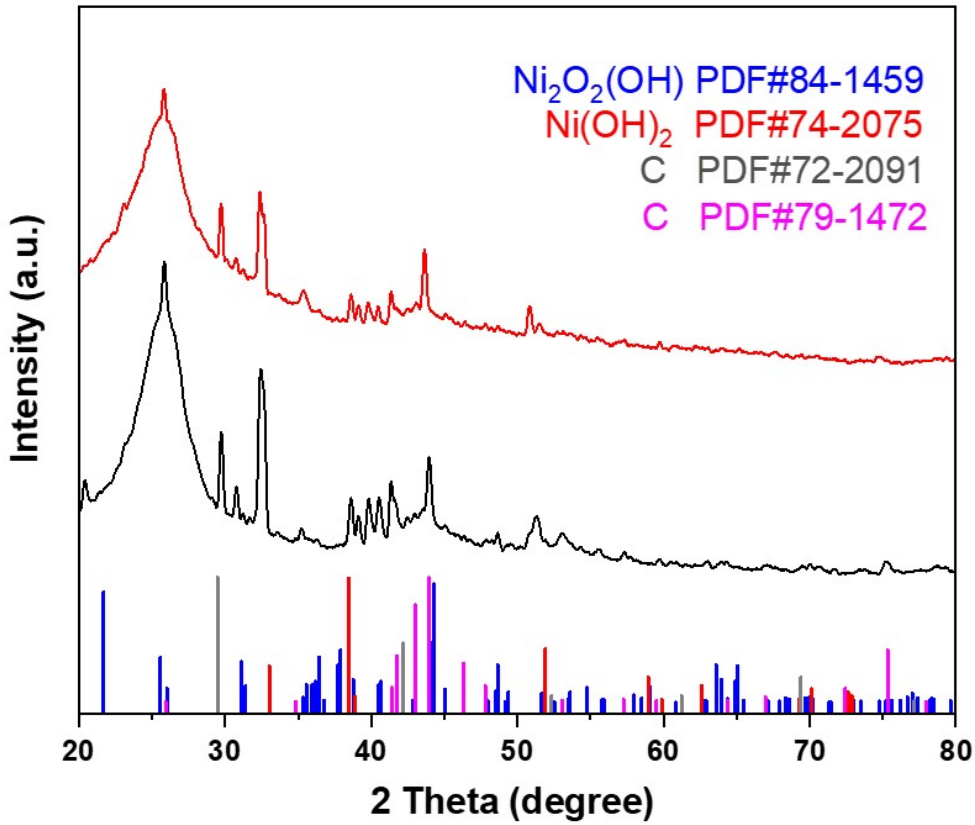

Figure S9. XRD results of (a) Ni@PMMA-BM and Ni@PBT-BM after CV cycles

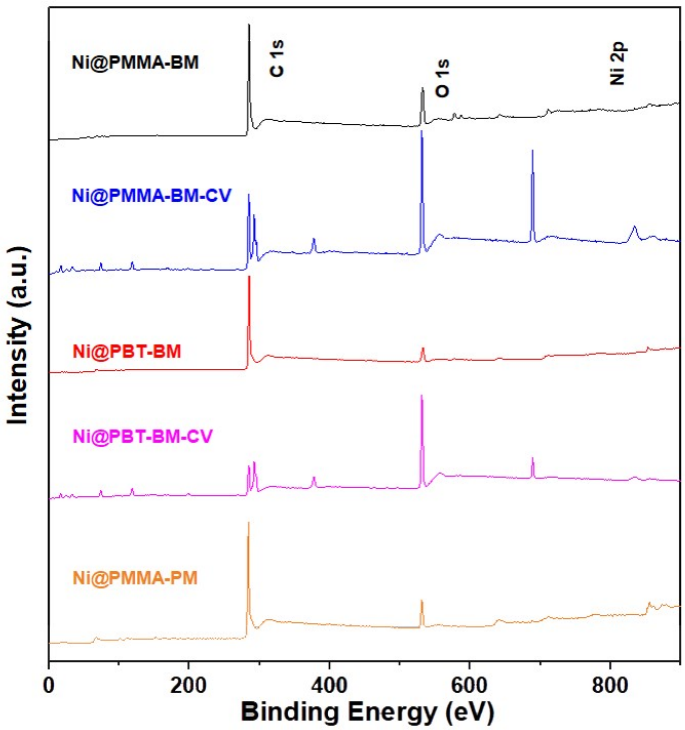

Figure S10. XPS survey spectra of Ni@PMMA-BM, Ni@PMMA-BM-CV, Ni@PBT-BM, Ni@PBT-BM-CV and Ni@PMMA-PM.

Tables

Table S1. Summary Nitrogen absorption and desorption report of as-prepared samples.

Catalysts	**Ni@PMMA-BM**	**Ni@PBT-BM**	**Fe@PMMA-BM**	**Mn@PBT-BM**	**Co@PBT-BM**	**Ni@C**	**Ni_xO_y**
BET Surface Area (m^2/g)	62	156	72	62	121	274	0
Pore size (nm)	6.7	14.3	14.7	15.7	23.5	7.85	-
Pore volume (cm^3/g)	0.04	0.43	0.22	0.17	0.27	0.23	-

Table S2. Element contents of the samples via ICP and XPS results.

	ICP (wt%)	**XPS (wt%)**
Ni@PMMA-BM	26.03%	4.5%
Ni@PBT-BM	23.21%	5.1%

Table S3. Comparison of the OER performance of Ni@PMMA-PM catalyst with other reported OER catalysts.

	Material	The loading weight (mg/cm^2)	Overpotential/mV at 10 mA cm^{-2})	Ref.
1	NFC@CNSs	2	256	Surfaces and Interfaces, 2021, 26, 101361
2	NiFe-LDH/FeSoy-CNSs-A	0.04	300	Nano Res. 14, 1175–1186 (2021)
3	NiCoFe-NC	0.04	250	Small 2018, 14, 1801878
4	Mo_2C/Co@NC	1	308	Appl. Catal. B 2021, 296, 120360
5	Co@C/NC	0.4	300	Energy Fuels 2022, 36, 1688–1696
6	MnxOy/N-doped carbon	0.07	450	Angewandte Chemie International Edition, 2014, 53, 8508-8512
7	$Co(OH)_2$@g-C_3N_4	0.07	320	J. Mater. Chem. A, 2016,4, 12940-12946
8	Co_3O_4/P-CN	0.57	320	ACS Appl. Energy Mater. 2019, 2, 4718–4729
9	Ni@Ru/CNS-10%	0.357	356	Electrochimica Acta, 2019, 320, 134568
10	Co_3O_4/N-doped-graphene	0.07	320	Nat Mater, 2011, 10, 780-786
11	$NiCoSe_2$-x/NC	4.54	300	Electrochimica Acta, 2018, 272, 161-168
12	BN/CA-NiCoFe-600	0.255	321	Journal of Colloid and Interface Science, 2022, 613, 126-135
13	Ni SAs@S/N-CMF	1.9	285	Adv. Mater. 2022, 34, 2203442
14	$Co_2N_{0.67}$-BHPC	0.3	340	Journal of Energy Chemistry, 2021, 54, 626-638
14	S/N-CMF@$Fe_xCo_yNi_{1-x-y}$-MOF	7.5	296	Adv. Mater. 2023, 35, 2207888
15	Ni@PMMA-PM	0.5	263	This work

Table S4. Surface atomic ratio of as-made samples determined by XPS.

Catalysts	**Atomic %**		
	C	O	Ni
Ni@PMMA-BM	81.86	17.20	0.94
Ni@PMMA-BM-CV	53.82	44.47	1.71
Ni@PBT-BM	90.22	8.64	1.14
Ni@PBT-BM-CV	39.45	59.52	1.03
Ni@PMMA-PM	87.37	9.79	2.84